J. Fluid Mech. (2002), *vol.* 461, *pp.* 51–60.
DOI: 10.1017/S0022112002008595 Printed in the United Kingdom

Pipe flow measurements over a wide range of Reynolds numbers using liquid helium and various gases

By CHRIS J. SWANSON[1], BRIAN JULIAN[1], GARY G. IHAS[2] AND RUSSELL J. DONNELLY[1]

[1]Cryogenic Helium Turbulence Laboratory, Department of Physics, University of Oregon, Eugene, Oregon 97403, USA

[2]Department of Physics, University of Florida, Gainesville, Florida, 32611, USA

(Received 21 July 2001 and in revised form 23 January 2002)

We demonstrate that an unusually small pipe flow apparatus using both liquid helium and room temperature gases can span an enormous range of Reynolds numbers. This paper describes the construction and operation of the apparatus in some detail. A wide range of Reynolds numbers is an advantage in any experiment seeking to establish scaling laws. This experiment also adds to evidence already in hand that the normal phase of liquid helium is a Navier–Stokes fluid. Finally, we explore recent questions concerning the influence of molecular motions on the transition to turbulence (Muriel 1998) and are unable to observe any influence.

1. Introduction

Very high Reynolds and Rayleigh number flows using cryogenic helium are achievable in relatively small (1 m high and smaller) facilities (Niemela *et al.* 2000; Chanal *et al.* 2000; Chavanne *et al.* 1997; Moisy, Tabeling & Willaime 1999; Fuzier & Van Sciver 2001). Building even larger ($\sim$ 10 m high) cryogenic facilities increases the range of Reynolds and Rayleigh numbers beyond those achievable using other working fluids (Donnelly 1991; Donnelly & Sreenivasan 1998). Furthermore, there are many types of measurement which offer distinct advantages at low temperatures, such as thermometry (Lipa 1998), direct measurement of mean vorticity (Stalp, Skrbek & Donnelly 1999), hot-wire anemometry (Chanal *et al.* 1997, Emsellem *et al.* 1997, Swanson, Hall & Donnelly 2001), surface stress probing, and differential pressure determination (Swanson, Johnson & Donnelly 1998). In this paper we report the development of low-temperature measurement tools and the use of the normal phase of liquid helium (helium I) to reproduce standard friction factor measurements in fully developed flow in a pipe. Gaseous helium, nitrogen, oxygen, carbon dioxide, and sulphur hexafluoride are also used to obtain the widest range of Reynolds numbers ever achieved in a single pipe flow apparatus.

2. Experimental overview

We sought to make accurate measurements spanning a broad range of Reynolds numbers in a very small apparatus. The emphasis is on attaining the highest Reynolds numbers using cryogenic helium. Using a flow pipe only 28 cm long and 0.4672 cm in diameter we were able to span a Reynolds number range from 10 to 10^6 by taking

	ρ (kg m^{-3})	μ (Pa s)	ν (m^2 s^{-1})	Re	ΔP (Pa)
Helium gas	0.16	1.97×10^{-5}	123×10^{-6}	190	7.3
O_2	1.29	2.05×10^{-5}	15.9×10^{-6}	1470	7.4
N_2	1.13	1.76×10^{-5}	15.6×10^{-6}	1500	6.5
CO_2	1.77	1.49×10^{-5}	8.42×10^{-6}	2780	5.5
SF_6	5.90	1.51×10^{-5}	2.56×10^{-6}	9120	24.6
Helium I	125	0.324×10^{-5}	0.026×10^{-6}	900 000	202

TABLE 1. Fluids used, with density, viscosity, kinematic viscosity, Reynolds number and pressure drop across taps 5 cm apart. Both Re and ΔP were calculated at a mean flow velocity of 5 m s^{-1}. All gases were held at room temperature and helium I was held at 4.2 K.

advantage of the variation in the kinematic viscosity of the fluids used. Fluids that were used together with some associated parameters are listed in table 1.

The flow through the pipe is generated by a controlled compression of a metal bellows attached to the mouth of the pipe. The pressure gradient generated by the flow is measured near the exit of the pipe with two static pressure taps a distance L apart. From the mean velocity and the pressure gradient across the taps, we can determine the friction factor λ given by

$$\lambda = \frac{D}{L} \frac{\Delta P}{\frac{1}{2}\rho V^2} \tag{2.1}$$

where D is the diameter of the pipe, ΔP is the pressure drop over the distance L, the fluid density is ρ, and the mean fluid velocity is V. A schematic drawing of the apparatus is shown in figure 1. While figure 1 is not to scale, it does give an idea of the scale of apparatus, which is located at the bottom of a standard open-bath pumped cryostat, available from any of a number of vendors. After a measurement, the bellows is refilled by retracting the push rod, pulling fluid back up the pipe. The bellows and motor are capable of sustaining a maximum flow of 10 m s^{-1} for 9 s, and for much longer at lower speeds.

Our experimental arrangement is flexible enough to allow us to use both helium I at 4.2 K and a variety of gases at room temperature. Because of the cryogenic thermal insulation of the dewar, the temperatures of the gases at room temperature are extremely stable after settling overnight. We estimate that at room temperature the apparatus has a thermal time constant on the order of 12 hours.

In order to operate with room temperature gas, the following protocol was adopted. The dewar was pumped and flushed twice with the working fluid to ensure that there were no contaminants. The system was then allowed to rest overnight so that the temperature of the gas could come to equilibrium. The pressure of the dewar is maintained at the pressure of the room by placing a large airtight bag over one of the dewar ports. This was found to be necessary since the movement of the drive shaft into the dewar steadily raised the pressure during the run if the dewar volume was kept constant. Operation in liquid helium was essentially identical except a larger bag was used to collect the boil-off of the liquid helium. By keeping the liquid at atmospheric pressure, we were able to maintain a constant temperature at saturated vapour pressure.

Substantial effort was made to ensure the pipe was hydraulically smooth. We started with an electropolished stainless steel tube. However, the electropolishing process only

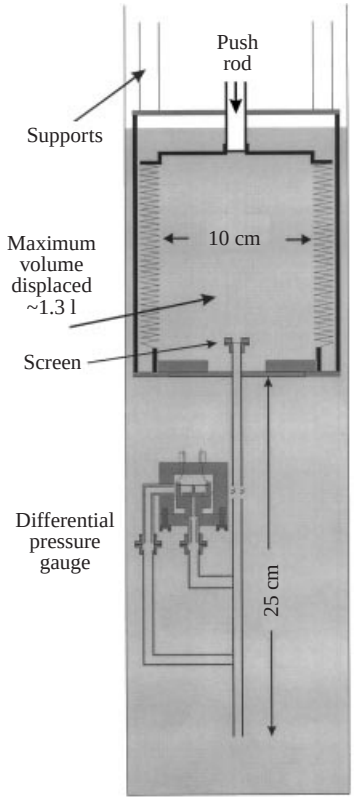

FIGURE 1. Schematic diagram of the pipe flow apparatus (not to scale)

smooths the pipe walls on a very small scale, leaving larger scale variations untouched. To further smooth the walls a hone with 0.05 μm polishing grit was passed through the pipe for a period of two days. Inspection by means of a microscope of the inside of the tube subsequent to the polishing showed scratches of approximately 0.05 μm with occasional scratches of order 0.5 μm. These rare scratches were probably due to fine dust particles which became mixed into the polishing grit. We adopt a smoothness criterion that the r.m.s. roughness, k, be less than a few viscous wall units, namely

$$\frac{k}{d} \leqslant \frac{2}{Re\sqrt{\lambda/8}}. \tag{2.2}$$

For a Reynolds number of 2×10^6 this corresponds to $k \leqslant 0.1\,\mu$m. Assuming the r.m.s. average depth of scratches to be slightly less than the width we may consider our pipe to be smooth at this Reynolds number.

The mean diameter was also carefully measured. Although we could not easily measure the inner diameter throughout the length of the tube, the outer diameter was constant to within 10 microns. We could, however, measure the inside diameter in short sections cut from the original tubing. Measurements prior to and subsequent to the polishing process showed no perceptible changes in the diameter. Thus we believe the diameter to be 0.4672 ± 0.0010 cm.

Because the pipe is so small, the pressure taps were also small, requiring care to be taken to make taps free of burrs. First a small hole was drilled part way into the wall, leaving 0.29 mm of wall thickness. Through this thinner wall, a smaller hole of

0.25 mm diameter was made using EDM. This technique electro-chemically etches a hole leaving no burr. To determine the shape of the hole we examined a similarly made hole under 80X magnification. We found this hole to be symmetric with no evidence of a burr or rounding at the edge. Since the pressure taps were identical, we expect errors in the measurement of differential pressure to be insignificant.

The entrance to the pipe is covered by a small screen to enhance the development of the turbulent flow and reduce large-scale flow. The screen is 62% open and has 12.6 meshes per cm giving approximately 5 wires across the diameter of the inlet. The pipe exit is located approximately 11 diameters from the lower pressure tap hole (see figure 1).

3. Pressure measurements

Measured quantities were pressure, temperature, pressure drop and mean velocity. The pressure and temperature of the gases were measured to an accuracy of 0.1%. From these values we could calculate the density of the gas from the virial equation of state and the viscosity from tables (Weast 2000 and Dymond & Smith 1980). For liquid helium, density and viscosity were obtained from tables (HEPAK, software from Cryodata, Inc.).

The mean velocity of the flow was determined as follows. A DC linear servo-controlled motor outside the cryostat drives a custom-built actuator. The frequency of the motor is measured with an encoder and counter during each push of the bellows. The actuator propels a long shaft into the dewar through an O-ring seal. The shaft velocity is proportional to the volumetric flow rate out of the bellows with the constant of proportionality determined by a calibration using water. The final flow velocity is then calculated from the measured diameter of the pipe. Thus we have

$$\overline{V} = \frac{\alpha f p}{\pi d^2} \tag{3.1}$$

where α is the calibrated volume change per unit length of stroke, f is the frequency of the motor, p is the pitch of the actuator thread, and d is the diameter of the flow tube.

The pressure drop was determined by measuring the differential pressure between the static pressure taps located 5 cm apart. The differential pressure was measured with a capacitance-type gauge connected to these taps (Swanson *et al.* 1998). The gauge has a linear response over a pressure range from 0 to 1000 Pa, and performs equally well at room temperature and at liquid helium temperatures. It also maintains its calibration upon thermal cycling, and is insensitive to changes in temperature, absolute pressure or mounting strains. The capacitance is measured with an AC capacitance bridge and lock-in amplifier allowing us to span seven orders of magnitude in capacitance. The minimum resolution was about 2×10^{-6} pF $\mathrm{Hz}^{-1/2}$ corresponding to 0.02 Pa $\mathrm{Hz}^{-1/2}$.

Typical measurements of pressure as a function of time for helium I are shown in figure 2. The top line corresponds to the capacitance measured without flow. Each drop in the capacitance corresponds to a differential pressure applied to the gauge by the flow. The flow velocities in the pipe for each push of the bellows are indicated.

The uncertainty in the measurement of friction factor and Reynolds number can be evaluated as follows. For the Reynolds number the uncertainty is a combination of uncertainty in velocity of 0.8%, in diameter of 0.3% and properties of the fluid. For the room temperature gases we estimate our uncertainty in v to be about 0.4% and for helium about 1%. Thus we estimate the total uncertainty in Re to be 1%

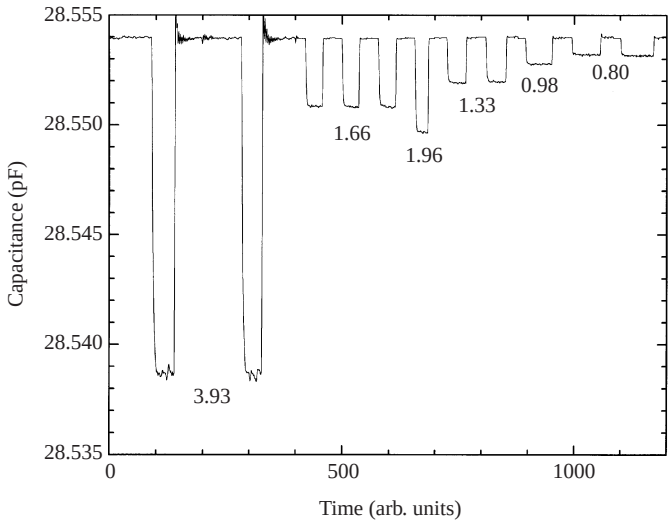

FIGURE 2. Capacitance response to flow rates ($\mathrm{m\,s^{-1}}$) indicated below the traces

for room temperature gases and 1.5% for helium. The uncertainty in the friction factor is slightly higher. Uncertainty in velocity is one source of uncertainty, especially since λ depends on the velocity squared. Another uncertainty comes from the static calibration of our pressure transducer based on three separate calibrations against an MKS Baratron pressure standard, which we estimate to be 0.5%. The most difficult uncertainty to account for is due to dynamic effects. Of particular concern is variation of the capacitance from changes in temperature and pressure of the fluid inside the capacitor. Changes in T and P affect the dielectric constant and consequently the capacitance. The best measure of these effects is perhaps the scatter in the data. For the room temperature gases the scatter is around 2% and for the helium data around 4%.

4. Results

Friction factor as a function of Reynolds number is plotted in figure 3. Figure 3(a) shows our measurements and figure 3(b) shows the measurements from numerous water experiments, including those of Nikuradse. To emphasize the reduction in the size of the apparatus we have achieved, the two devices are shown to scale in figure 4.

In figure 3(a) the solid lines represent the accepted value of λ. In the laminar region, $\lambda = 64/Re$ and in the turbulent region the line is a combination of the equation of Blasius, $\lambda = 0.3164/Re^{1/4}$ and the recent results of Zagarola & Smits (1998). The agreement is good over the entire range of Re including the highest range where liquid helium is used. The only discrepancy occurs over a Reynolds number range from 800 to 2700, where we see a marked deviation from the solid line. This deviation is due to the fact that in this range the flow is not fully developed.

The entry lengths for a fully developed pressure gradient differ considerably between laminar and turbulent flow. In laminar flow the centreline velocity is within 1% of maximum at a position equal to $Re/15$ diameters from the entrance (Schlichting 1979). For our pipe with an entrance length of 38 diameters, we expect the centreline velocity to be within 1% of maximum for $Re<570$ and 5% of maximum for $Re<880$.

We found that the undeveloped flow did have an effect on our pressure drop measurements in laminar flow for Re of 800 and above. Figure 5 shows per cent

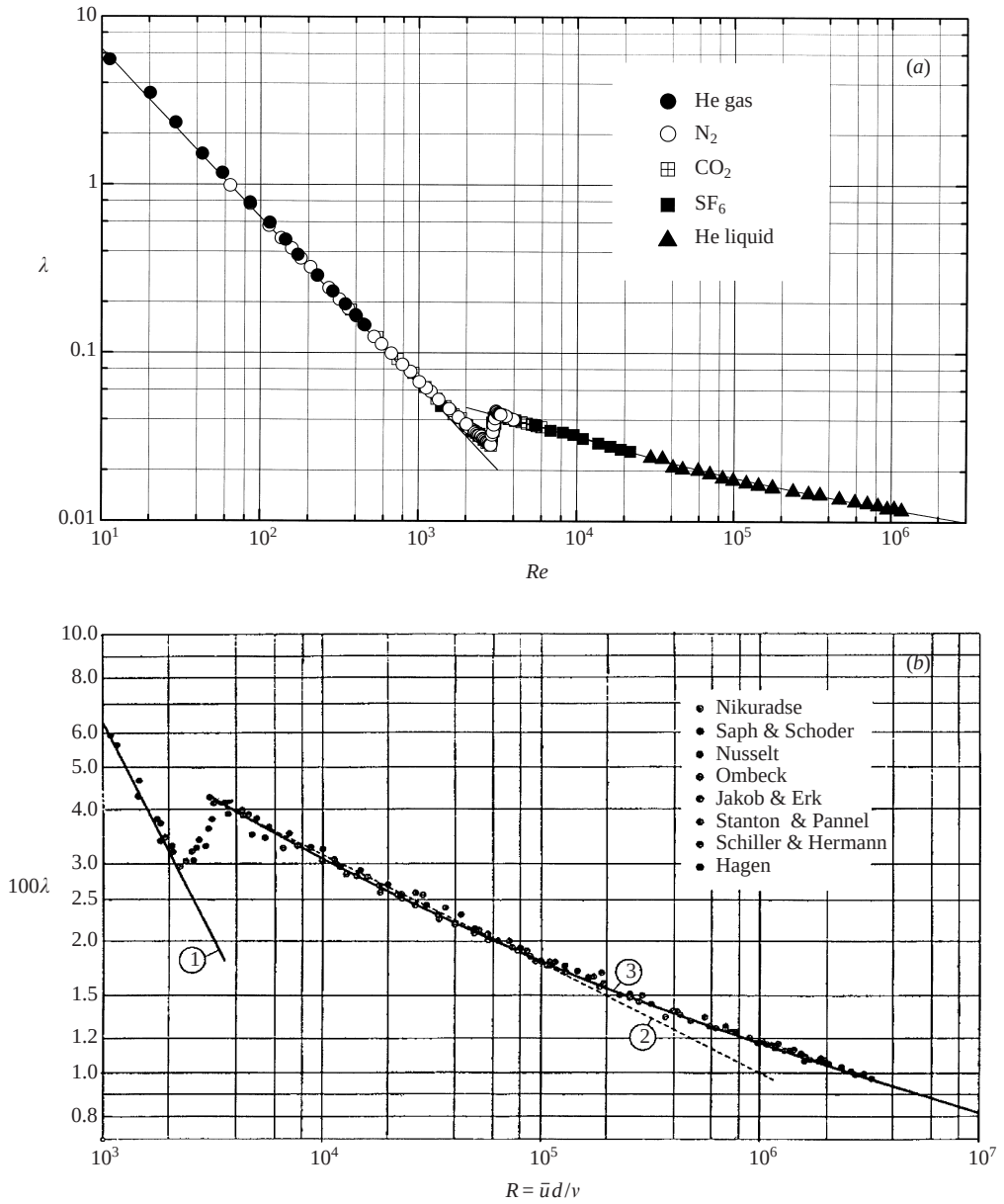

FIGURE 3. Friction factor as a function of Re: (a) present measurements for various gases and liquid helium in the present apparatus. (b) Friction factor as reproduced from Schlichting (1979). This celebrated figure shows the friction factor as deduced from the data of eight authors. Note that the lowest Reynolds number is above 1000. The circled numbers refer to different approximations discussed by Schlichting. The apparatus of Nikuradse weighed some tens of tons, to be compared to the apparatus of figure 1.

differences between friction factor measurements and the exact solution $\lambda = 64/Re$. To confirm that the short entry length was responsible we compared forward flow with an entry length of 38 diameters to backward flow with an entry length of 11 diameters. The squares in figure 5 represent flow moving forward down the pipe and the crossed circles represent flow moving backwards. In forward flow there is a

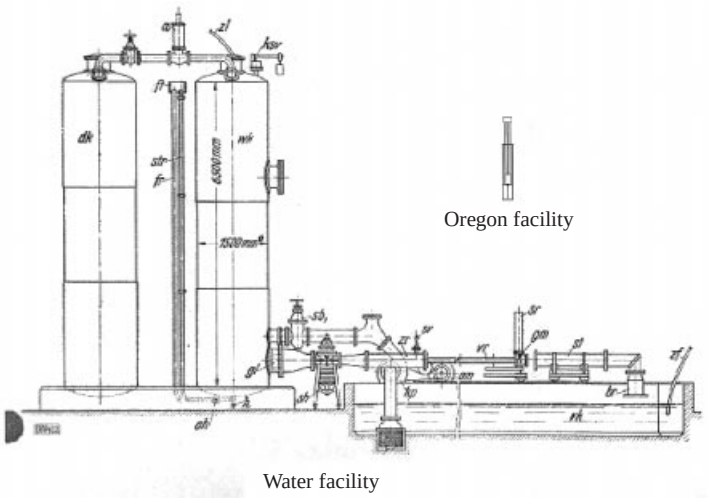

FIGURE 4. Scale drawing of the water facility used by Nikuradse and that used for our measurements.

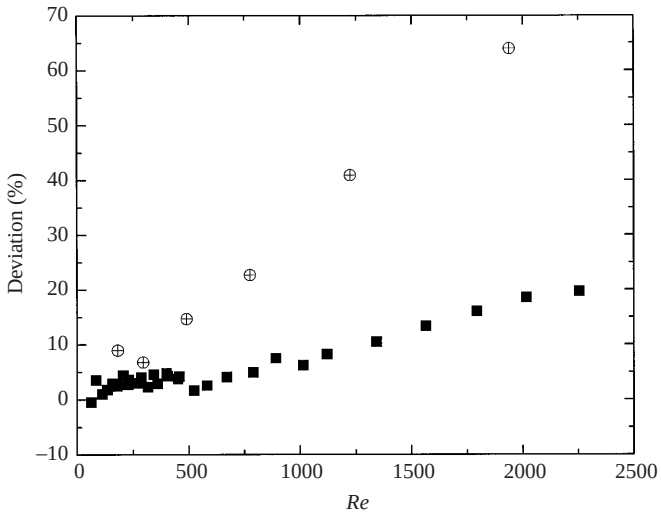

FIGURE 5. Deviations in friction factor, $100(\lambda_{meas} - \lambda_{calc})/\lambda_{calc}$ for flow down the pipe (solid squares) compared to flow up the pipe (crossed circles). The two cases have different entry lengths.

departure from the expected laminar flow line near a Reynolds number of around 800 as expected. To create backward flow we simply made measurements on the return stroke of the bellows. Because the entry length is only 11 diameters for backward flow we see a pronounced departure from the expected laminar flow curve at lower Reynolds number.

For turbulent flow the pressure gradient becomes fully developed much more quickly. It has been shown, for instance, that for $Re = 388\,000$ the pressure gradient is fully developed after only 15 diameters (Barbin 1961). It has been suggested that the entry length for fully developed turbulent flow in a pipe is given by $L/D \approx 0.5/\lambda + 5/\lambda^{1/2}$ (Zagarola & Smits 1998). For $Re = 388\,000$ this criterion would lead to an entry length of 78 diameters. However, the mean pressure gradient develops after

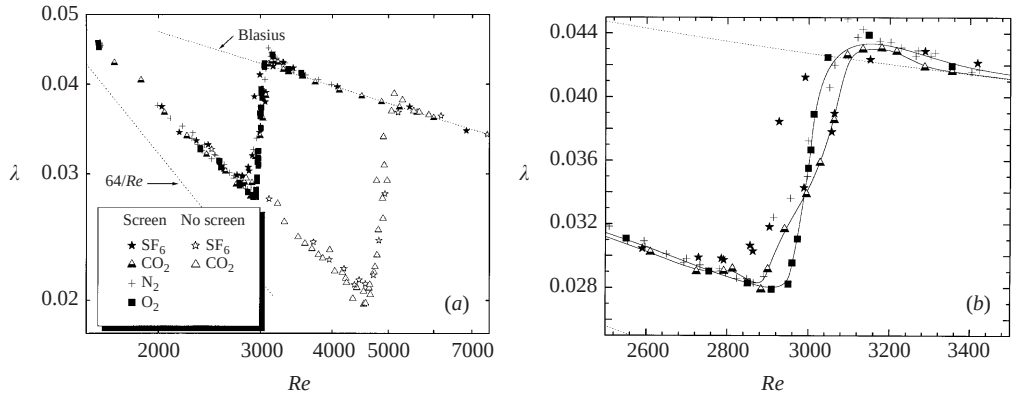

FIGURE 6. λ vs. Re near the transition to turbulence: (a) both entrance conditions as described in the text and (b) an expanded view of the larger Reynolds number transition. The lines are simply guides for the eye.

only 15 diameters at this Re. Even if the entry length for the mean pressure gradient grew as λ^{-1}, we would find, based on the results of Barbin, that at $Re = 2\,000\,000$ the entry length is only 20 diameters. Thus we believe that the mean pressure gradient is fully developed for all Reynolds numbers above the transition.

5. Transition to turbulence

Recently there have been theoretical suggestions that the transition to turbulence in a pipe depends not only on entry geometry and Reynolds number but also on the microscopic motions of the molecules (Muriel 1998). There has been experimental evidence that has both supported (Nerushev & Novopashin 1997; Novopashin & Muriel 1998, 2000) and refuted these claims (White & Sreenivasan 1998). Because of the adaptability of our apparatus to different gases we were able to explore these issues with some precision.

To study the transition we modified the entry geometry in case the predicted molecular effects could be more easily seen with a smoother entrance. Initially we used the screen at the entrance to the pipe as previously discussed. Later we removed the screen, allowing the flow to enter the pipe undisturbed. Upon removal of the screen the critical Reynolds number increased by 60%. This dependence of the critical Reynolds number on the initial conditions is not a surprising effect, and has been well studied (e.g. by Wygnanski & Champagne 1973). As a consequence, gases with lower kinematic viscosity remained laminar even at the highest flow speeds so that only CO_2 and SF_6 could be compared.

Data for both entry geometries are shown in figure 6(a), with an expanded view of one of the transitions in figure 6(b). In figure 6(b) we have drawn lines between some of the points as a visual aid. It is clear that the entrance condition has an enormous impact on the critical Reynolds number for transition as expected. It also appears that the type of gas does not.

We have defined the critical Reynolds number, Re_{crit}, as the Reynolds number at which the friction factor first changes slope. The results are shown in table 2. The third column indicates our measured percentage differences between Re_{crit} for CO_2 and that of other gases. The fourth column shows the percentage differences proposed

Gas	Re_{crit}	$\Delta Re/Re$ measured (%)	$\Delta Re/Re$ proposed (%)	B ($cm^3\ mol^{-1}$)
Screen entrance				
N_2	2870 ± 20	-0.7	$+13.4$	-0.6
O_2	2940 ± 10	$+1.7$	$+12.3$	-1.7
CO_2	2890 ± 20	–	–	-14
SF_6	2820 ± 50	-2.4	-18	-31.9
Open entrance				
CO_2	4660 ± 40	–	–	-14
SF_6	4650 ± 30	-0.2	-18	-31.9

TABLE 2. Results of measurements of the turbulent transition with various gases

in the article by Novopashin & Muriel (2000, equation 3), namely

$$\Delta Re/Re = \alpha n B \tag{5.1}$$

where $\alpha \approx 25$ is a dimensionless constant, n is the number of moles per unit volume, and B is the second virial coefficient. While there are some measured differences between the different gases they are much smaller than the proposed differences and do not seem to correspond with them. It is interesting to note that the Reynolds number at which the friction factor rises to halfway between the laminar value and the turbulent value is the same, to within 1% for all of the gases, provided the initial conditions are the same.

6. Future directions

We have shown that flow in liquid helium I can be considered on the same basis as any simple fluid. The conditions that lead to turbulence are similar, and the friction developed in flowing helium is, within statistical error, exactly the same as measured in water or compressed air. Because of the nature of low-temperature apparatus, measurements such as pressure and temperature may be made routinely with sufficient precision and stability for probing hydrodynamic questions. Other kinds of apparatus can also be envisioned using liquid and gaseous helium to achieve very high Reynolds and Rayleigh numbers. Some details of such apparatus are contained in Donnelly (1991) and Donnelly & Sreenivasan (1998).

We are grateful to Katepalli Sreenivasan, Alexander Smits, Mark Zagarola, and Amador Muriel for useful discussions. This research was supported by the United States National Science Foundation under grant DMR95-29609.

REFERENCES

BARBIN, A. R. 1961 Development of turbulence in the inlet of a smooth pipe. PhD thesis, Purdue University.

CHANAL, O., BAGUENARD, B., BETHOUX, A. O. &, CHABAUD, B. 1997 Micronic-size cryogenic thermometer for turbulence measurements. *Rev. Sci. Instrum.* **68**, 2442–2446.

CHANAL, O., CHABAUD, B., CASTAING, B. &, HEBRAL, B. 2000 Intermittency in a turbulent low temperature gaseous helium jet. *Eur. Phys. J.* B **17**, 309–317.

Chavanne, X., Chilla, F., Castaing, B., Hebral, B., Chabaud, B. & Chaussy, J. 1997 Observation of the ultimate regime in Rayleigh–Benard convection. *Phys. Rev. Lett*. **79**, 3648–3651.

Donnelly, R. J. (Ed). 1991 *High Reynolds Number Flows Using Liquid and Gaseous Helium*. Springer.

Donnelly, R. J. & Sreenivasan, K. R. (Eds). 1998 *Flow at Ultra-high Reynolds and Rayleigh Numbers*. Springer.

Dymond, J. H. & Smith, E. B. 1980 *The Virial Coefficients of Pure Gases and Mixtures: a Critical Compilation*. Clarendon.

Emsellem, V., Kadanoff, L.P., Lohse, D., Tabeling, P. & Wang, Z.J. 1997 Transitions and probes in turbulent helium *Phys. Rev*. E **55**, 2672–2681.

Fuzier, S. & Van Sciver, S. W. 2001 Steady state pressure drop and heat transfer in He II forced flow at high Reynolds number. *Cryogenics* **41**, 453–458.

Lipa, J. 1998 Cryogenic thermometry for turbulence research: an overview. In *Flow at Ultra-high Reynolds and Rayleigh Numbers* (ed. R. J. Donnelly & K. R. Sreenivasan). Springer.

Moisy, F., Tabeling, P. & Willaime, H. 1999 Kolmogorov equation in a fully developed turbulence experiment. *Phys. Rev. Lett*. **82**, 3994–3997.

Muriel, A. 1998 Quantum kinetic model of turbulence. *Physica* D **124**, 225–247.

Nerushev, O. A. & Novopashin, S. A. 1997 Rotational relaxation and transition to turbulence. *Phys. Lett*. A **232**, 243–245.

Niemela, J. J., Skrbek, L., Sreenivasan, K. R. & Donnelly, R. J. 2000 Turbulent convection at very high Rayleigh numbers. *Nature* **404**, 837–840.

Novopashin, S. A. & Muriel, A. 1998 Anomalous transition to turbulence in inert gases. *JETP Lett*. **68**, 582–584.

Novopashin, S. A. & Muriel, A. 2000 A statistical criterion for the onset of turbulence. *Tech. Phys. Lett*. **26**, 231–232.

Schlichting, H. 1979 *Boundary Layer Theory*, 7th Edn. McGraw-Hill.

Stalp, S. R., Skrbek, L. & Donnelly, R. J. 1999 Decay of grid turbulence in a finite channel. *Phys. Rev. Lett*. **82**, 4831–4834.

Swanson, C. J., Hall, S. C. & Donnelly, R. J. 2001 Measurement devices for cryogenic turbulence research. *Cryogenics* **41**, 341–345.

Swanson, C. J., Johnson, K. & Donnelly, R. J. 1998 An accurate differential pressure gauge for use in liquid and gaseous helium. *Cryogenics* **38**, 673–677.

Weast, R. C. (Ed.) 2000 *Handbook of Chemistry and Physics*, 81st Edn. CRC Press.

White C. M. & Sreenivasan, K. R. 1998 Does molecular rotation affect the transition Reynolds number? *Phys. Lett*. A **238**, 323–327.

Wygnanski, I. J. & Champagne, F. H. 1973 On transition in a pipe. I. The origin of puffs and slugs and the flow in a turbulent slug. *J. Fluid Mech*. **59**, 281–335.

Zagarola, M. V. & Smits, A. J. 1998 Mean-flow scaling of turbulent pipe flow. *J. Fluid Mech*. **373**, 33–79.